Vol 11 No 6, June 2002
1009-1963/2002/11(06)/0601-07

Chinese Physics

© 2002 Chin. Phys. Soc.
and IOP Publishing Ltd

Optical responses of dilute anisotropic composites: numerical calculations via Green's function formalism

Gu Ying(古 英)[a)b)] and Yu Kin-Wah(余建华)[b)]

[a)] *State Key Laboratory for Mesoscopic Physics & Department of Physics, Peking University, Beijing* 100871, *China*

[b)] *Department of Physics, the Chinese University of Hong Kong, Shatin, New Territories, Hong Kong, China*

(Received 23 November 2001; revised manuscript received 8 January 2002)

We investigate the linear and nonlinear optical responses of dilute anisotropic networks using Green's function formalism [Gu Y *et al* 1999 *Phys. Rev.* B **59** 12847]. For different applied fields, numerical calculations indicate that a large third-order nonlinear enhancement and a broad infrared absorption arise from the geometric anisotropy. We also show the overlap and separation between the absorption peak and nonlinear enhancement peak when the applied field is parallel and perpendicular to the anisotropy, respectively. The results can be understood in terms of the inverse participation ratios with $q = 2$ and the spectral distribution of optical responses.

Keywords: response to electromagnetic fields, composites
PACC: 7430G, 8160H

1. Introduction

Recently, the optical properties of composites have aroused great interest. In order to open new possibilities in information processing and transmission, a large optical nonlinearity may be desirable.[1] Composite materials, especially small metal particles and metal clusters on the nanometre scale embedded in a dielectric host exhibit a strong nonlinear optical enhancement through the inhomogeneous local field and geometric response effects.[1−5] It is also known that these composites give rise to an anomalously large absorption in the infrared spectrum.[6−8] To analyse the optical responses, it is more convenient to adopt the spectral representation.[9] For various anisotropic composites, the spectral density was calculated as a function of volume fractions $p_{\|}$ and $p_{\perp}$ by the effective medium approximation (EMA).[2,10,11] A large nonlinear optical enhancement, as well as the separation of the absorption peak from the nonlinear enhancement peak, has been found. By EMA, the fluctuation of the local field has been averaged out. So it is difficult to find the physical origins of the optical enhancement and the separation of optical peaks. In this connection, Green's function formalism (GFF) was developed to deal with the optical responses of the arbitrary-shaped metallic clusters embedded in an infinite dielectric network at the quasistatic limit.[12,13] Using the formalism, the resonance spectrum and local field distribution for each eigenmode can be analytically obtained. The aim of this paper is to investigate the linear and nonlinear optical responses of the dilute anisotropic networks in view of the local field distribution.

In the following, a binary dilute anisotropy network is considered. We use the random number generator to produce the geometric anisotropy. The metallic bonds parallel to the applied field are assigned with the fraction $p_{\|}$, and the metallic bonds perpendicular to the applied field with $p_{\perp}$. In dilute systems, the condition, $p_{\|} \times p_{\perp} = 0.01$, is satisfied. When we change $p_{\|}$ from 0.1 to 0.8, the corresponding $p_{\perp}$ varies from 0.1 to 0.0125. In section 2, the Green's functions for the effective linear response ϵ_{e} and effective nonlinear response χ_{e} are derived. In section 3, the inverse participation ratios (IPR) with $q = 2$ are used to represent the localized and extended eigenstates in anisotropic networks. In section 4, the spectra of the absorption and the third-order nonlinear enhancement are illustrated. When the applied field is parallel to the anisotropy of the networks, the overlap of the absorption peak with the nonlinear enhancement peak is found within the interval $0.1 < p_{\|} < 0.8$. In contrast, for the perpendicular applied field, the separation of the absorption peak from the nonlinear enhancement peak is enhanced when the anisotropy $p_{\|}$ is increased.

These results are explained in section 3, numerically confirmed in section 4, and concluded in section 5.

2. Effective linear and nonlinear responses

Consider an infinite binary network as shown in Fig.1, where the impurity bonds with admittance ϵ_1 are employed to replace the bonds in an otherwise homogeneous network of identical admittance ϵ_2. The admittance of each bond is generally complex and frequency-dependent. All the impurity bonds construct the cluster subspace. When resonance occurs, the potential of the joint points can be computed by the GFF. Instead of the point source $\delta_{x,0}$,[12] the source term is replaced by ρ_x at the point x. Hence, in the subspace, $\tilde{V}$ is a linear combination of the right eigenvector $\tilde{R}$ of Green's matrix M

$$\tilde{V} = \sum_{n=1}^{n_s} \frac{s}{\epsilon_2(s-s_n)} \sum_{y\in C} \left(\tilde{L}_{n,y} \sum_{x'} \rho_{x'} \tilde{G}_{y,x'} \right) \tilde{R}_n. \quad (1)$$

And for the site $x(x_1, x_2)$ outside the cluster, V_x becomes

$$V_x = \sum_{x'} \rho_{x'} \tilde{G}_{x,x'} + \sum_{n=1}^{n_s} \frac{1}{\epsilon_2(s-s_n)} \times \sum_{y\in C} \left(\tilde{L}_{n,y} \sum_{x'} \rho_{x'} \tilde{G}_{y,x'} \right) \sum_{z\in C} M_{x,z} \tilde{R}_{n,z}. \quad (2)$$

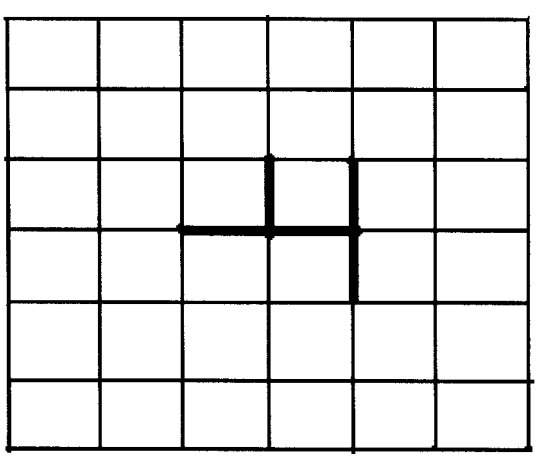


Fig.1. Schematic diagram of a cluster (shown by thick lines) embedded in an infinite network.

In the uniform field E_0 along the 1 direction, $\tilde{V}$ reads

$$\tilde{V} = \sum_{n=1}^{n_s} \frac{sE_0}{\epsilon_2(s-s_n)} \left(\sum_{y\in C} \tilde{L}_{n,y} y_1 \right) \tilde{R}_n. \quad (3)$$

For a binary network with $N \times N$ square lattices, in the quasistatic limit, the displacement $\boldsymbol{D}$ of the ith bond is related to the local field $\boldsymbol{E}$ by the relation $\boldsymbol{D} = \epsilon_i \boldsymbol{E} + \chi_i |\boldsymbol{E}|^2 \boldsymbol{E}$,[14] where ϵ_i is the dielectric constant and χ_i is the third-order nonlinear susceptibility of the bond. Parameters ϵ_i, χ_i are set to be $\epsilon_1,\ \chi_1$ for the impurity bonds, and $\epsilon_2,\ \chi_2$ for the matrix bonds. By the finite difference transformation, the effective linear response along the applied field is

$$\epsilon_e E_0 = \sum_{(x,y)\in C} \frac{\epsilon_1 (V_x - V_y)}{a} + \sum_{(x',y')\notin C} \frac{\epsilon_2 (V_{x'} - V_{y'})}{a} \quad (4)$$

with the magnitude of field $E_0 = 1$ and lattice constant $a = 1$, where $(x, y) \in C$ means that x and y are the nearest neighbours in the same cluster while $(x', y') \notin C$ means x' and y' are the nearest neighbours but not in the same cluster. When we employ $N(N+1)\epsilon_2 = \sum_{x,y} \epsilon_2 (V_x - V_y)$, $\epsilon_2 - \epsilon_e$ can be expressed by the points within the cluster subspace as

$$N(N+1)\epsilon_2 - \epsilon_e = \sum_{(x,y)\in C} (\epsilon_2 - \epsilon_1)(V_x - V_y). \quad (5)$$

Here $\epsilon_1/\epsilon_2 = (s-1)/s$, so we have

$$N(N+1) - \frac{\epsilon_e}{\epsilon_2} = \sum_{n=1}^{n_s} \frac{1}{\epsilon_2(s-s_n)} \left(\sum_{y\in C} \tilde{L}_{n,y} y_1 \right) \times \sum_{(x,y)\in C} (x_1 - y_1)(\tilde{R}_{n,x} - \tilde{R}_{n,y}). \quad (6)$$

Because x and y are neighbours, the values of $x_1 - y_1$ can be only $+1$ or -1. Physically, the absorption along the applied field is larger than that found perpendicular to the applied field. In the following calculations, ϵ_e always represents the absorption along the applied field. For simplicity, we let $L_{\hat{n}} = \sum_{y\in C} \tilde{L}_{n,y} y_1$, $R_{\hat{n}} = \sum_{x,y\in C} (x_1 - y_1)(\tilde{R}_{n,x} - \tilde{R}_{n,y})$, and $\gamma_n = L_{\hat{n}} R_{\hat{n}}$. The imaginary part of ϵ_e corresponding to the absorption is

$$-\mathrm{Im}(\epsilon_e) = \mathrm{Im} \sum_{n=1}^{n_s} \frac{\gamma_n}{\epsilon_2(s-s_n)}, \quad (7)$$

and γ_n, referred to as the cross section, obeys the sum rule[15]

$$\sum_n \gamma_n = N_h, \quad (8)$$

where N_h is the number of horizontal bonds along the applied field.

Since the local fields are determined completely, our formulae can be used to calculate the nonlinear response. By relating the total electrostatic energy to the effective coefficients, the third-order nonlinearity $\chi'_{\rm e}$ is defined by[14]

$$\int_v \boldsymbol{D}(x)\dot{\boldsymbol{E}}(x) = V[\epsilon'_{\rm e}\overline{\boldsymbol{E}}^2 + \chi'_{\rm e}\overline{\boldsymbol{E}}^4], \tag{9}$$

where $\overline{\boldsymbol{E}} = (1/V)\int_v \boldsymbol{E}(x)\mathrm{d}^3x$ is the space averaged electric field. For infinite networks, $\overline{\boldsymbol{E}} = \boldsymbol{E}_0 = 1$ and the nonlinear response function is given by[10]

$$\chi'_{\rm e} = \frac{1}{l^2}\sum_i \chi_i |\delta v_i|^2 {\delta v_i}^2, \tag{10}$$

where the summation is over all bonds and δv_i is the (general complex) potential difference across the bond i and for a two-dimensional case, $V = l^2$. When all the bonds have a nonlinear term, i.e. $\chi_1 = \chi_2 = 1.0$, with the lattice constant $a = 1$, the effective nonlinear response is written as

$$\chi_{\rm e} = V\chi'_{\rm e} = \sum_{(x,y)} |V_x - V_y|^2 (V_x - V_y)^2. \tag{11}$$

The third-order nonlinearity $\chi_{\rm e}$ is expressed as the summation of the fourth moment of local electric field. So the fluctuation of the local electric field enhances the nonlinear optical responses.

3. Inverse participation ratios with $q = 2$

First, the IPR of eigenvectors of Green's matrix M in the eigensystem with n_s joint points are defined. The nth normalized right eigenvector is

$$R_n = \{R_{n,1},\ \ldots,\ R_{n,i},\ \ldots R_{n,n_s}\} \tag{12}$$

with $< R_n >= 0$ and $< {R_n}^2 >= 1$. The IPR of R_n is written as[16]

$$\mathrm{IPR}(R_n) = \sum_{i=1}^{n_s} {R_{n,i}}^{2q}, \tag{13}$$

where $q = 2$. The calculation of $\mathrm{IPR}(R_n)$ is limited in the nontrivial eigenstates. The number of $\mathrm{IPR}(R_n)$ is equal to or less than n_s. In the above Eqs.(1) and (2), it is found that the right eigenvectors of M are closely related to the local fields of the impurity cluster in the subspace. So the IPR can be used to represent the localization of the eigenstates. The IPR amplify the profiles of eigenstates, namely, the localized states become more pronounced and extended states become smoother. Hence, the larger values of IPR always correspond to the stronger optical responses. This is verified in the following sections.

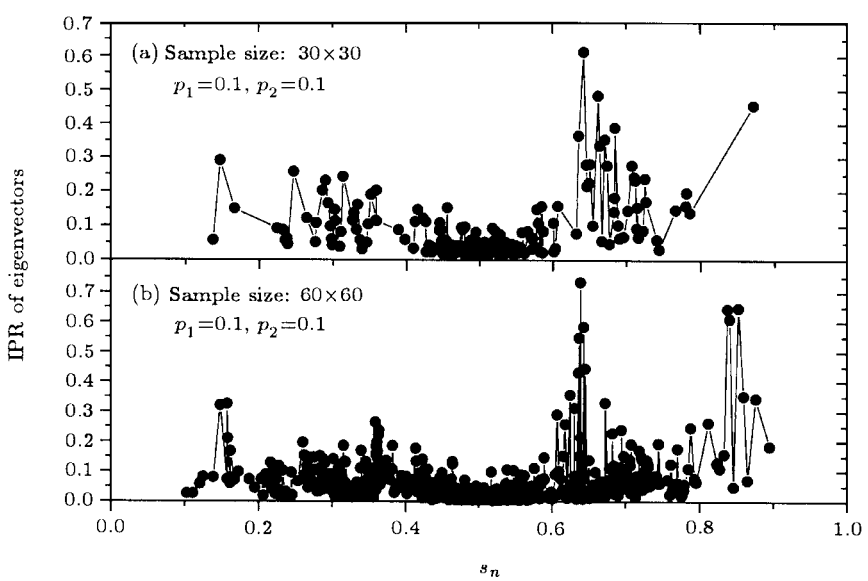


Fig.2. Size effect of IPR of right eigenvectors for two samples: 30×30 and 60×60. Here $p_{\|} = p_1 = 0.1$, $p_{\perp} = p_2 = 0.1$.

To consider the size effect, the IPR in the dilute isotropic composites with $p_{\parallel} = 0.1$ and $p_{\perp} = 0.1$ are shown in Fig.2. In this figure, two samples have sizes of 30×30 and 60×60. The peaks represent the localized states and the valleys correspond to the extended states. Comparing the distribution of peaks and valleys in two samples, we find that the size effect is not very obvious. It is also seen that the density of state is larger around $s = 0.5$ than that around $s = 0.0$ or $s = 1.0$. The localized states incline to accumulate $s = 0.0$ or $s = 1.0$, while the extended states are near $s = 0.5$. So there exists a duality about $s = 0.5$.[13] The high values of IPR imply the strong optical responses at $s = 0.0$ or $s = 1.0$.

Figure 3 displays the IPR of the dilute anisotropic systems. We know that the resonance spectrum is very sensitive to the microstructure.[13] For each case, comparing two samples, we see that the peaks of IPR are very stable though their microstructure is completely different. So in the following, for the definite parameters $p_{\parallel}$ and $p_{\perp}$, it is reasonable to investigate the optical responses using only one sample. When the anisotropy is increased from Fig.3(a) to Fig.3(g), the localized states incline towards $s = 0.0$ or $s = 1.0$. The distributions of localized and extended states have roughly the same feature as that in the isotropic case, i.e. we find more localized states at $s = 0.0$ and $s = 1.0$ than at $s = 0.5$, but denser at $s = 0.5$. The distribution of IPR is caused purely by the morphology of the sample. In the next section, we discuss how the different applied fields act on the optical responses when the geometric anisotropy is increased.

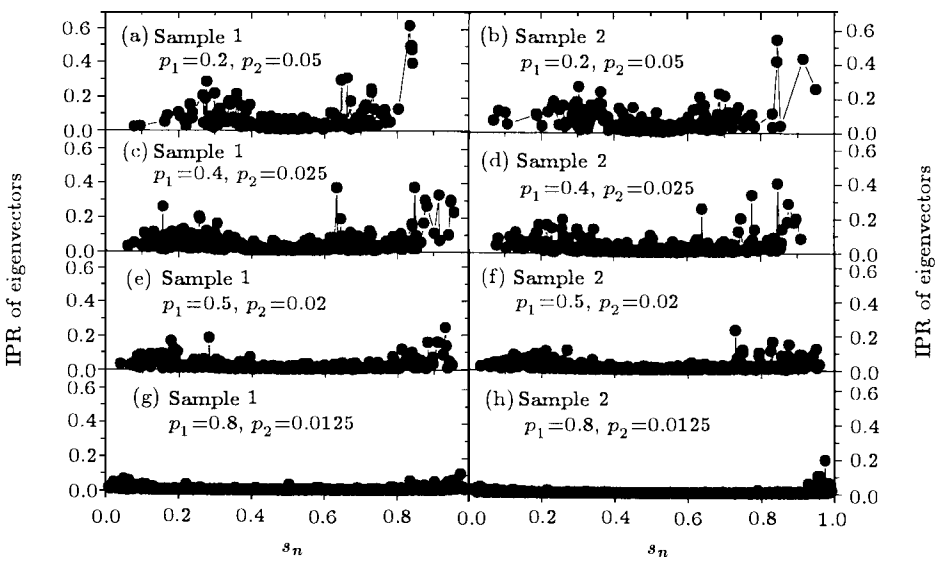


Fig.3. IPR of right eigenvectors of the dilute anisotropic systems. Samples 1 and 2 are randomly chosen. In (a) and (b), $p_{\parallel} = p_1 = 0.2$, $p_{\perp} = p_2 = 0.05$; in (c) and (d), $p_{\parallel} = p_1 = 0.4$, $p_{\perp} = p_2 = 0.025$; in (e) and (f), $p_{\parallel} = p_1 = 0.5$, $p_{\perp} = p_2 = 0.02$; in (g) and (h), $p_{\parallel} = p_1 = 0.8$, $p_{\perp} = p_2 = 0.0125$.

4. Spectra of absorption and third-order nonlinear enhancement

The optical responses can be properly described by the absorption spectrum γ_n and the third-order nonlinear enhancement spectrum as shown in Figs.4 and 5. When the applied field is parallel to the direction of anisotropy, it well affects the optical properties. The envelopes of the absorption and third-order nonlinear enhancements become narrower and the intensity is more enhanced with the increasing anisotropy. The main optical peaks are ranged in the interval $s \in [0.5, 0.6]$, which correspond to the dipolar approximation. In this figure, we cannot find the separation of the absorption peak from the third-order nonlinear enhancement peak. The results of the single sample conflict with those of previous works.[13] The reason is that the EMA has averaged out the fluctuation of the local field, which plays a central role for the effective optical responses. At $s = 0.5$, the density of localized states is much smaller than that of extended states. The optical properties of the specific sample are determined by its own eigenstates, not by "effective medium". So it is not reasonable for all of the cases to express the optical properties of one

specific sample only by the same macroscopic parameters $p_{\|}$ and $p_{\perp}$. In Fig.5, when the applied field is perpendicular to the anisotropy, the optical responses of the dilute anisotropic samples are plotted. It is seen that the peaks of absorption are redshifted while the peaks of the third-order nonlinear enhancement are blueshifted when the anisotropy is added. There is a larger peak separation with increasing geometric anisotropy. For all the applied fields, it is natural to find a large third-order nonlinear enhancement and a broad infrared absorption because the localized states exist in the whole resonant area. The separation of optical peaks is found only for the perpendicular applied field.

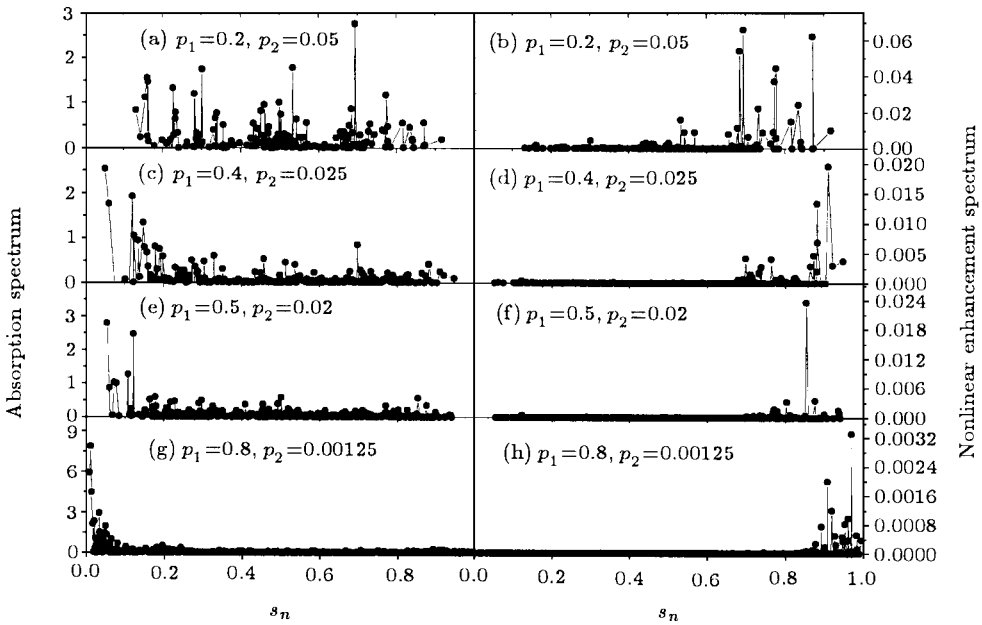


Fig.4. Spectra of the absorption and the third-order nonlinear enhancement of dilute anisotropic systems for the parallel applied field. In (a) and (b), $p_{\|} = p_1 = 0.2$, $p_{\perp} = p_2 = 0.05$; in (c) and (d), $p_{\|} = p_1 = 0.4$, $p_{\perp} = p_2 = 0.025$; in (e) and (f), $p_{\|} = p_1 = 0.5$, $p_{\perp} = p_2 = 0.02$; in (g) and (h), $p_{\|} = p_1 = 0.8$, $p_{\perp} = p_2 = 0.0125$.

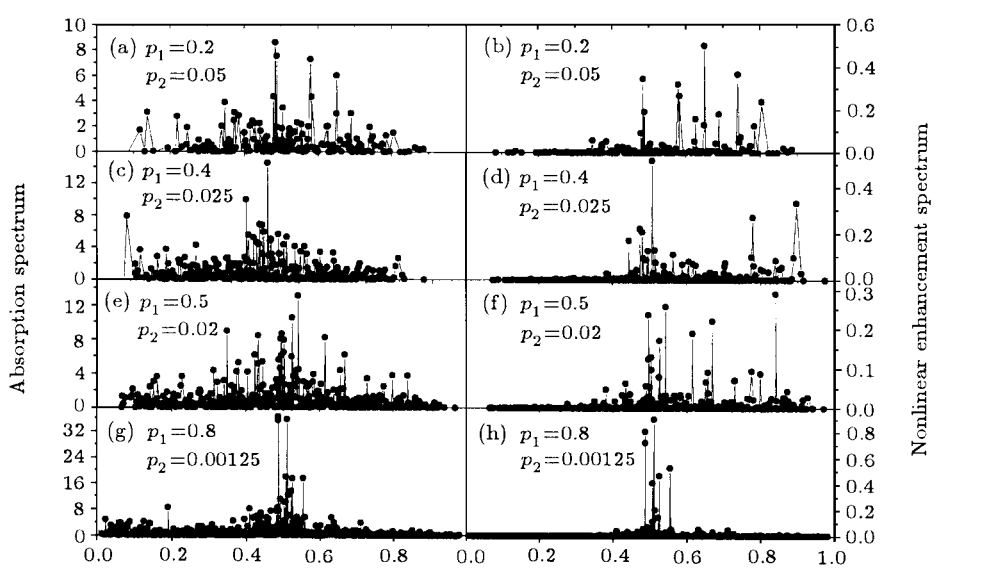


Fig.5. Spectra of the absorption and the third-order nonlinear enhancement of dilute anisotropic systems for the perpendicular applied field. In (a) and (b), $p_{\|} = p_1 = 0.2$, $p_{\perp} = p_2 = 0.05$; in (c) and (d), $p_{\|} = p_1 = 0.4$, $p_{\perp} = p_2 = 0.025$; in (e) and (f), $p_{\|} = p_1 = 0.5$, $p_{\perp} = p_2 = 0.02$; in (g) and (h), $p_{\|} = p_1 = 0.8$, $p_{\perp} = p_2 = 0.0125$.

Then, the Drude free electronic model is employed to calculate the optical properties of the dilute anisotropic composites. The admittance of the impurity metallic bonds is

$$\epsilon_1 = 1 - \frac{\omega_p^2}{\omega(\omega + i\gamma)}, \tag{14}$$

where ω_p is the plasma frequency, and γ is a damping constant. For metal, the plasma frequency ω_p is 10^{16}, being in the ultraviolet. We choose $\gamma = 0.1\omega_p$, which is the typical value of a metal, and $\epsilon_2 = 1.77$, which is the dielectric constant of water for model calculations. The range of optical responses is $\omega/\omega_p \in (0, 1)$.

Optical responses of various anisotropic networks are illustrated in Fig.6. The nonlinear enhancement χ_e is divided by 150 for the comparison with the linear absorption. The direction of anisotropy in Figs.6(a), (c), (e) and (g) is parallel to the applied field. The peak at $\omega/\omega_p = 0.6$ corresponds to the dipolar approximation of the whole system. In these figures, the separation of the absorption peak and the nonlinear enhancement peak is not found, as observed in Fig.4. Note that this result is different from that of previous works.[2,10,11] However, when the applied field is perpendicular to the anisotropy, as shown in Figs.6(b), (d), (f) and (h), in each of the figures both the separation of linear and nonlinear peaks, and the third-order nonlinear enhancement are seen.

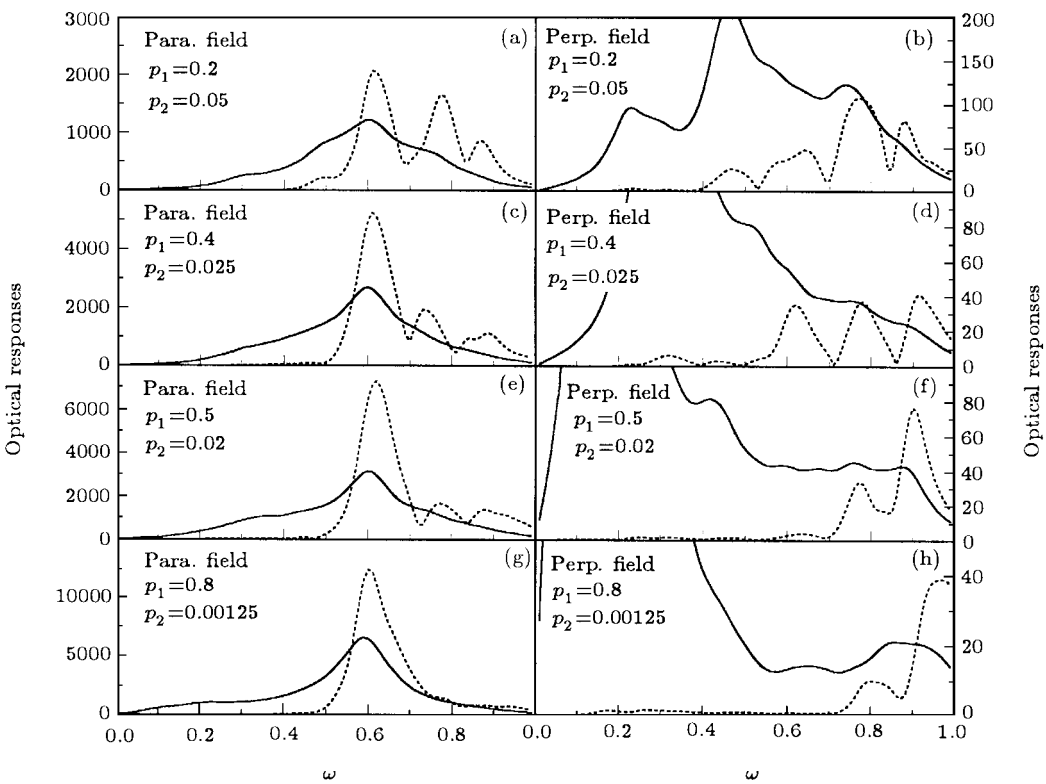


Fig.6. Linear and nonlinear optical responses of the dilute anisotropic systems by the Drude model. Para.field means that the applied field is parallel to the anisotropy while perp.field denotes that the applied field is perpendicular to the anisotropy. The solid curves represent the imaginary part of ϵ_e, or the absorption. The dotted curves are the third-order nonlinear enhancement $\chi_e/150$. Here p_1 corresponds to $p_{\parallel}$ in the text and p_2 is $p_{\perp}$.

5. Discussion and conclusions

In this paper, the optical responses of dilute binary anisotropic networks are investigated numerically by the GFF. Green's functions for the effective linear and nonlinear responses are derived. The IPR with $q = 2$ are given to describe the localization and extension of eigenstates. The spectra of the absorption and the third-order nonlinear enhancement are exhibited for the different applied fields. We also compute the optical responses for the Drude model. For the dilute anisotropic networks, we conclude the following.

1. The size effect of the optical responses is not obvious.

2. The IPR with $q = 2$ can be used to represent

the localization and extension of eigenstates.

3. The wide optical absorption and large nonlinear enhancement are caused by the geometric anisotropy.

4. The peaks of the absorption and nonlinear enhancement overlap when the applied field is parallel to the anisotropy. While, for the perpendicular applied field, the absorption peak is separated from the nonlinear enhancement peak.

5. The structure sensitivity does not affect the main optical properties, but the details of optical responses.

From points 2,3 and 4 above and from previous works,[2,10,11] geometric anisotropy is the main reason to enhance the optical responses. For a specific sample, when the different fields are applied, the positions of optical responses do not vary, but the local field distributions are quite different. Therefore the optical properties of resonant composites are determined by the geometric anisotropy, as well as by the applied sources.

Acknowledgment

Gu Y acknowledges the useful discussions with Professor Yang Z R.

References

[1] See articles in: Bowden C M and Haus J W (ed) *J. Opt. Soc. Am.* B **6** (a Special Issue on Nonlinear-Optical Properties of Materials)
[2] Yuen K P, Law M F, Yu K W and Sheng P 1997 *Phys. Rev.* E **56** R1322
[3] See articles in: Shalave V M 1997 *Nanostructured Materials: Clusters, Composites and Thin Films, ACS Symposium Series* **679** (American Chemical Society)
[4] Siu W H and Yu K W 1996 *Phys. Rev.* B **53** 9277
[5] Wei E B and Gu G Q 2000 *Chin. Phys.* **9** 464
[6] Tanner D B, Sievers A J and Buhrman R A 1975 *Phys. Rev.* B **11** 1330
[7] Granqvist C G, Buhrman R A, Wyns J and Sievers A J 1976 *Phys. Rev. Lett.* **37** 625
[8] Devaty R P and Sievers A J 1984 *Phys. Rev. Lett.* **52** 1344
[9] Bergman D J and Stroud D 1992 *Solid State Phys.* **146** 147
[10] Law M F, Gu Y and Yu K W 1998 *Phys. Rev.* B **58** 12536
[11] Law M F, Gu Y and Yu K W 1998 *J. Phys.: Condens. Matter* **10** 9549
[12] Gu Y, Yu K W and Sun H 1999 *Phys. Rev.* B **59** 12847
[13] Gu Y 2001 *Ph D Thesis* (copyrighted by the Chinese University of Hong Kong (CUHK))
[14] Yu K W, Hui P M and Stroud D 1993 *Phys. Rev.* B **47** 4150
[15] Clerc J P, Giraud G, Luck J M and Robin Th 1996 *J. Phys. A: Math. Gen.* **29** 4781
[16] Wegner F 1980 *Z. Phys.* B **36** 209